

# First detection of ultra-high energy emission from gamma-ray binary LS I +61° 303

Zhen Cao,<sup>1,2,3</sup> F. Aharonian,<sup>3,4,5,6</sup> Y.X. Bai,<sup>1,3</sup> Y.W. Bao,<sup>7</sup> D. Bastieri,<sup>8</sup> X.J. Bi,<sup>1,2,3</sup> Y.J. Bi,<sup>1,3</sup> W. Bian,<sup>7</sup> A.V. Bukevich,<sup>9</sup> C.M. Cai,<sup>10</sup> W.Y. Cao,<sup>4</sup> Zhe Cao,<sup>11,4</sup> J. Chang,<sup>12</sup> J.F. Chang,<sup>1,3,11</sup> A.M. Chen,<sup>7</sup> E.S. Chen,<sup>1,3</sup> G.H. Chen,<sup>8</sup> H.X. Chen,<sup>13</sup> Liang Chen,<sup>14</sup> Long Chen,<sup>10</sup> M.J. Chen,<sup>1,3</sup> M.L. Chen,<sup>1,3,11</sup> Q.H. Chen,<sup>10</sup> S. Chen,<sup>15</sup> S.H. Chen,<sup>1,2,3</sup> S.Z. Chen,<sup>1,3</sup> T.L. Chen,<sup>16</sup> X.B. Chen,<sup>17</sup> X.J. Chen,<sup>10</sup> Y. Chen,<sup>17</sup> N. Cheng,<sup>1,3</sup> Y.D. Cheng,<sup>1,2,3</sup> M.C. Chu,<sup>18</sup> M.Y. Cui,<sup>12</sup> S.W. Cui,<sup>19</sup> X.H. Cui,<sup>20</sup> Y.D. Cui,<sup>21</sup> B.Z. Dai,<sup>15</sup> H.L. Dai,<sup>1,3,11</sup> Z.G. Dai,<sup>4</sup> Danzengluobu,<sup>16</sup> Y.X. Diao,<sup>10</sup> X.Q. Dong,<sup>1,2,3</sup> K.K. Duan,<sup>12</sup> J.H. Fan,<sup>8</sup> Y.Z. Fan,<sup>12</sup> J. Fang,<sup>15</sup> J.H. Fang,<sup>13</sup> K. Fang,<sup>1,3</sup> C.F. Feng,<sup>22</sup> H. Feng,<sup>1</sup> L. Feng,<sup>12</sup> S.H. Feng,<sup>1,3</sup> X.T. Feng,<sup>22</sup> Y. Feng,<sup>13</sup> Y.L. Feng,<sup>16</sup> S. Gabici,<sup>23</sup> B. Gao,<sup>1,3</sup> C.D. Gao,<sup>22</sup> Q. Gao,<sup>16</sup> W. Gao,<sup>1,3</sup> W.K. Gao,<sup>1,2,3</sup> M.M. Ge,<sup>15</sup> T.T. Ge,<sup>21</sup> L.S. Geng,<sup>1,3</sup> G. Giacinti,<sup>7</sup> G.H. Gong,<sup>24</sup> Q.B. Gou,<sup>1,3</sup> M.H. Gu,<sup>1,3,11</sup> F.L. Guo,<sup>14</sup> J. Guo,<sup>24</sup> X.L. Guo,<sup>10</sup> Y.Q. Guo,<sup>1,3</sup> Y.Y. Guo,<sup>12</sup> Y.A. Han,<sup>25</sup> O.A. Hannuksela,<sup>18</sup> M. Hasan,<sup>1,2,3</sup> H.H. He,<sup>1,2,3</sup> H.N. He,<sup>12</sup> J.Y. He,<sup>12</sup> X.Y. He,<sup>12</sup> Y. He,<sup>10</sup> S. Hernández-Cadena,<sup>7</sup> B.W. Hou,<sup>1,2,3</sup> C. Hou,<sup>1,3</sup> X. Hou,<sup>26</sup> H.B. Hu,<sup>1,2,3</sup> S.C. Hu,<sup>1,3,27</sup> C. Huang,<sup>17</sup> D.H. Huang,<sup>10</sup> J.J. Huang,<sup>1,2,3</sup> T.Q. Huang,<sup>1,3</sup> W.J. Huang,<sup>21</sup> X.T. Huang,<sup>22</sup> X.Y. Huang,<sup>12</sup> Y. Huang,<sup>1,3,27</sup> Y.Y. Huang,<sup>17</sup> X.L. Ji,<sup>1,3,11</sup> H.Y. Jia,<sup>10</sup> K. Jia,<sup>22</sup> H.B. Jiang,<sup>1,3</sup> K. Jiang,<sup>11,4</sup> X.W. Jiang,<sup>1,3</sup> Z.J. Jiang,<sup>15</sup> M. Jin,<sup>10</sup> S. Kaci,<sup>7</sup> M.M. Kang,<sup>28</sup> I. Karpikov,<sup>9</sup> D. Khangulyan,<sup>1,3</sup> D. Kuleshov,<sup>9</sup> K. Kurinov,<sup>9</sup> B.B. Li,<sup>19</sup> Cheng Li,<sup>11,4</sup> Cong Li,<sup>1,3</sup> D. Li,<sup>1,2,3</sup> F. Li,<sup>1,3,11</sup> H.B. Li,<sup>1,2,3</sup> H.C. Li,<sup>1,3</sup> Jian Li,<sup>4</sup> Jie Li,<sup>1,3,11</sup> K. Li,<sup>1,3</sup> L. Li,<sup>29</sup> R.L. Li,<sup>12</sup> S.D. Li,<sup>14,2</sup> T.Y. Li,<sup>7</sup> W.L. Li,<sup>7</sup> X.R. Li,<sup>1,3</sup> Xin Li,<sup>11,4</sup> Y. Li,<sup>7</sup> Y.Z. Li,<sup>1,2,3</sup> Zhe Li,<sup>1,3</sup> Zhuo Li,<sup>30</sup> E.W. Liang,<sup>31</sup> Y.F. Liang,<sup>31</sup> S.J. Lin,<sup>21</sup> B. Liu,<sup>12</sup> C. Liu,<sup>1,3</sup> D. Liu,<sup>22</sup> D.B. Liu,<sup>7</sup> H. Liu,<sup>10</sup> H.D. Liu,<sup>25</sup> J. Liu,<sup>1,3</sup> J.L. Liu,<sup>1,3</sup> J.R. Liu,<sup>10</sup> M.Y. Liu,<sup>16</sup> R.Y. Liu,<sup>17</sup> S.M. Liu,<sup>10</sup> W. Liu,<sup>1,3</sup> X. Liu,<sup>10</sup> Y. Liu,<sup>8</sup> Y. Liu,<sup>10</sup> Y.N. Liu,<sup>24</sup> Y.Q. Lou,<sup>24</sup> Q. Luo,<sup>21</sup> Y. Luo,<sup>7</sup> H.K. Lv,<sup>1,3</sup> B.Q. Ma,<sup>25,30</sup> L.L. Ma,<sup>1,3</sup> X.H. Ma,<sup>1,3</sup> J.R. Mao,<sup>26</sup> Z. Min,<sup>1,3</sup> W. Mitthumsiri,<sup>32</sup> G.B. Mou,<sup>33</sup> H.J. Mu,<sup>25</sup> A. Neronov,<sup>23</sup> K.C.Y. Ng,<sup>18</sup> M.Y. Ni,<sup>12</sup> L. Nie,<sup>10</sup> L.J. Ou,<sup>8</sup> P. Pattarakijwanich,<sup>32</sup> Z.Y. Pei,<sup>8</sup> J.C. Qi,<sup>1,2,3</sup> M.Y. Qi,<sup>1,3</sup> J.J. Qin,<sup>4</sup> A. Raza,<sup>1,2,3</sup> C.Y. Ren,<sup>12</sup> D. Ruffolo,<sup>32</sup> A. Sáiz,<sup>32</sup> D. Semikoz,<sup>23</sup> L. Shao,<sup>19</sup> O. Shchegolev,<sup>9,34</sup> Y.Z. Shen,<sup>17</sup> X.D. Sheng,<sup>1,3</sup> Z.D. Shi,<sup>4</sup> F.W. Shu,<sup>29</sup> H.C. Song,<sup>30</sup> Yu.V. Stenkin,<sup>9,34</sup> V. Stepanov,<sup>9</sup> Y. Su,<sup>12</sup> D.X. Sun,<sup>4,12</sup> H. Sun,<sup>22</sup> Q.N. Sun,<sup>1,3</sup> X.N. Sun,<sup>31</sup> Z.B. Sun,<sup>35</sup> N.H. Tabasam,<sup>22</sup> J. Takata,<sup>36</sup> P.H.T. Tam,<sup>21</sup> H.B. Tan,<sup>17</sup> Q.W. Tang,<sup>29</sup> R. Tang,<sup>7</sup> Z.B. Tang,<sup>11,4</sup> W.W. Tian,<sup>2,20</sup> C.N. Tong,<sup>17</sup> L.H. Wan,<sup>21</sup> C. Wang,<sup>35</sup> G.W. Wang,<sup>4</sup> H.G. Wang,<sup>8</sup> J.C. Wang,<sup>26</sup> K. Wang,<sup>30</sup> Kai Wang,<sup>17</sup> Kai Wang,<sup>36</sup> L.P. Wang,<sup>1,2,3</sup> L.Y. Wang,<sup>1,3</sup> L.Y. Wang,<sup>19</sup> R. Wang,<sup>22</sup> W. Wang,<sup>21</sup> X.G. Wang,<sup>31</sup> X.J. Wang,<sup>10</sup> X.Y. Wang,<sup>17</sup> Y. Wang,<sup>10</sup> Y.D. Wang,<sup>1,3</sup> Z.H. Wang,<sup>28</sup> Z.X. Wang,<sup>15</sup> Zheng Wang,<sup>1,3,11</sup> D.M. Wei,<sup>12</sup> J.J. Wei,<sup>12</sup> Y.J. Wei,<sup>1,2,3</sup> T. Wen,<sup>1,3</sup> S.S. Weng,<sup>33</sup> C.Y. Wu,<sup>1,3</sup> H.R. Wu,<sup>1,3</sup> Q.W. Wu,<sup>36</sup> S. Wu,<sup>1,3</sup> X.F. Wu,<sup>12</sup> Y.S. Wu,<sup>4</sup> S.Q. Xi,<sup>1,3</sup> J. Xia,<sup>4,12</sup> J.J. Xia,<sup>10</sup> G.M. Xiang,<sup>14,2</sup> D.X. Xiao,<sup>19</sup> G. Xiao,<sup>1,3</sup> Y.L. Xin,<sup>10</sup> Y. Xing,<sup>14</sup> D.R. Xiong,<sup>26</sup> Z. Xiong,<sup>1,2,3</sup> D.L. Xu,<sup>7</sup> R.F. Xu,<sup>1,2,3</sup> R.X. Xu,<sup>30</sup> W.L. Xu,<sup>28</sup> L. Xue,<sup>22</sup> D.H. Yan,<sup>15</sup> J.Z. Yan,<sup>12</sup> T. Yan,<sup>1,3</sup> C.W. Yang,<sup>28</sup> C.Y. Yang,<sup>26</sup> F.F. Yang,<sup>1,3,11</sup> L.L. Yang,<sup>21</sup> M.J. Yang,<sup>1,3</sup> R.Z. Yang,<sup>4</sup> W.X. Yang,<sup>8</sup> Z.H. Yang,<sup>7</sup> Z.G. Yao,<sup>1,3</sup> X.A. Ye,<sup>12</sup> L.Q. Yin,<sup>1,3</sup> N. Yin,<sup>22</sup> X.H. You,<sup>1,3</sup> Z.Y. You,<sup>1,3</sup> Q. Yuan,<sup>12</sup> H. Yue,<sup>1,2,3</sup> H.D. Zeng,<sup>12</sup> T.X. Zeng,<sup>1,3,11</sup> W. Zeng,<sup>15</sup> X.T. Zeng,<sup>21</sup> M. Zha,<sup>1,3</sup> B.B. Zhang,<sup>17</sup> B.T. Zhang,<sup>1,3</sup> C. Zhang,<sup>17</sup> F. Zhang,<sup>10</sup> H. Zhang,<sup>7</sup> H.M. Zhang,<sup>31</sup> H.Y. Zhang,<sup>15</sup> J.L. Zhang,<sup>20</sup> Li Zhang,<sup>15</sup> P.F. Zhang,<sup>15</sup> P.P. Zhang,<sup>4,12</sup> R. Zhang,<sup>12</sup> S.R. Zhang,<sup>19</sup> S.S. Zhang,<sup>1,3</sup> W.Y. Zhang,<sup>19</sup> X. Zhang,<sup>33</sup> X.P. Zhang,<sup>1,3</sup> Yi Zhang,<sup>1,12</sup> Yong Zhang,<sup>1,3</sup> Z.P. Zhang,<sup>4</sup> J. Zhao,<sup>1,3</sup> L. Zhao,<sup>11,4</sup> L.Z. Zhao,<sup>19</sup> S.P. Zhao,<sup>12</sup> X.H. Zhao,<sup>26</sup> Z.H. Zhao,<sup>4</sup> F. Zheng,<sup>35</sup> W.J. Zhong,<sup>17</sup> B. Zhou,<sup>1,3</sup> H. Zhou,<sup>7</sup> J.N. Zhou,<sup>14</sup> M. Zhou,<sup>29</sup> P. Zhou,<sup>17</sup> R. Zhou,<sup>28</sup> X.X. Zhou,<sup>1,2,3</sup> X.X. Zhou,<sup>10</sup> B.Y. Zhu,<sup>4,12</sup> C.G. Zhu,<sup>22</sup> F.R. Zhu,<sup>10</sup> H. Zhu,<sup>20</sup> K.J. Zhu,<sup>1,2,3,11</sup> Y.C. Zou,<sup>36</sup> and X. Zuo<sup>1,3</sup>

(The LHAASO Collaboration)\*

<sup>1</sup>Key Laboratory of Particle Astrophysics & Experimental Physics Division & Computing Center, Institute of High Energy Physics, Chinese Academy of Sciences, 100049 Beijing, China

<sup>2</sup>University of Chinese Academy of Sciences, 100049 Beijing, China

<sup>3</sup>TIANFU Cosmic Ray Research Center, Chengdu, Sichuan, China

<sup>4</sup>University of Science and Technology of China, 230026 Hefei, Anhui, China

<sup>5</sup>Yerevan State University, 1 Alek Manukyan Street, Yerevan 0025, Armenia

<sup>6</sup>Max-Planck-Institut für Nuklear Physik, P.O. Box 103980, 69029 Heidelberg, Germany

<sup>7</sup>Tsung-Dao Lee Institute & School of Physics and Astronomy, Shanghai Jiao Tong University, 200240 Shanghai, China

<sup>8</sup>Center for Astrophysics, Guangzhou University, 510006 Guangzhou, Guangdong, China

<sup>9</sup>Institute for Nuclear Research of Russian Academy of Sciences, 117312 Moscow, Russia

<sup>10</sup>School of Physical Science and Technology & School of Information Science and Technology, Southwest Jiaotong University, 610031 Chengdu, Sichuan, China

<sup>11</sup>State Key Laboratory of Particle Detection and Electronics, China

<sup>12</sup>Key Laboratory of Dark Matter and Space Astronomy & Key Laboratory of Radio Astronomy, Purple Mountain Observatory, Chinese Academy of Sciences, 210023 Nanjing, Jiangsu, China

- <sup>13</sup>Research Center for Astronomical Computing, Zhejiang Laboratory, 311121 Hangzhou, Zhejiang, China
- <sup>14</sup>Shanghai Astronomical Observatory, Chinese Academy of Sciences, 200030 Shanghai, China
- <sup>15</sup>School of Physics and Astronomy, Yunnan University, 650091 Kunming, Yunnan, China
- <sup>16</sup>Key Laboratory of Cosmic Rays (Tibet University),  
Ministry of Education, 850000 Lhasa, Tibet, China
- <sup>17</sup>School of Astronomy and Space Science, Nanjing University, 210023 Nanjing, Jiangsu, China
- <sup>18</sup>Department of Physics, The Chinese University of Hong Kong, Shatin, New Territories, Hong Kong, China
- <sup>19</sup>Hebei Normal University, 050024 Shijiazhuang, Hebei, China
- <sup>20</sup>Key Laboratory of Radio Astronomy and Technology,  
National Astronomical Observatories, Chinese Academy of Sciences, 100101 Beijing, China
- <sup>21</sup>School of Physics and Astronomy (Zhuhai) & School of Physics (Guangzhou)  
& Sino-French Institute of Nuclear Engineering and Technology (Zhuhai),  
Sun Yat-sen University, 519000 Zhuhai & 510275 Guangzhou, Guangdong, China
- <sup>22</sup>Institute of Frontier and Interdisciplinary Science,  
Shandong University, 266237 Qingdao, Shandong, China
- <sup>23</sup>APC, Université Paris Cité, CNRS/IN2P3, CEA/IRFU, Observatoire de Paris, 119 75205 Paris, France
- <sup>24</sup>Department of Engineering Physics & Department of Physics &  
Department of Astronomy, Tsinghua University, 100084 Beijing, China
- <sup>25</sup>School of Physics and Microelectronics, Zhengzhou University, 450001 Zhengzhou, Henan, China
- <sup>26</sup>Yunnan Observatories, Chinese Academy of Sciences, 650216 Kunming, Yunnan, China
- <sup>27</sup>China Center of Advanced Science and Technology, Beijing 100190, China
- <sup>28</sup>College of Physics, Sichuan University, 610065 Chengdu, Sichuan, China
- <sup>29</sup>Center for Relativistic Astrophysics and High Energy Physics,  
School of Physics and Materials Science & Institute of Space Science and Technology,  
Nanchang University, 330031 Nanchang, Jiangxi, China
- <sup>30</sup>School of Physics & Kavli Institute for Astronomy and Astrophysics, Peking University, 100871 Beijing, China
- <sup>31</sup>Guangxi Key Laboratory for Relativistic Astrophysics,  
School of Physical Science and Technology, Guangxi University, 530004 Nanning, Guangxi, China
- <sup>32</sup>Department of Physics, Faculty of Science, Mahidol University, Bangkok 10400, Thailand
- <sup>33</sup>School of Physics and Technology, Nanjing Normal University, 210023 Nanjing, Jiangsu, China
- <sup>34</sup>Moscow Institute of Physics and Technology, 141700 Moscow, Russia
- <sup>35</sup>National Space Science Center, Chinese Academy of Sciences, 100190 Beijing, China
- <sup>36</sup>School of Physics, Huazhong University of Science and Technology, Wuhan 430074, Hubei, China

We report the first detection of gamma-ray emission up to ultra-high-energy (UHE;  $>100$  TeV) emission from the prototypical gamma-ray binary system LS I +61° 303 using data from the Large High Altitude Air Shower Observatory (LHAASO). It is detected with significances of  $9.2\sigma$  in WCDA (1.4–30.5 TeV) and  $6.2\sigma$  in KM2A (25–267 TeV); in KM2A alone we identify 16 photon-like events above 100 TeV against an estimated 5.1 background events, corresponding to a  $3.8\sigma$  detection. These results provide compelling evidence of extreme particle acceleration in LS I +61° 303. Furthermore, we observe orbital modulation at  $4.0\sigma$  confidence between 25 and 100 TeV, and a hint of energy-dependent orbital modulation. These features can be understood in a composite scenario in which leptonic and hadronic processes jointly contribute.

## I. INTRODUCTION

Binary systems are prominent sources in the high-energy sky above a few keV, with X-ray binaries being the dominant population [1]. However, only a small number of these systems have been observed at more energetic gamma-ray bands [2, 3]. Among them, a distinct class known as gamma-ray binaries has been identified, characterized by persistent gamma-ray emission and spectral energy distributions ( $\nu F_\nu$ ) that peak in the gamma-ray range [2, 4]. All known gamma-ray binaries consist of a compact object in orbit around a massive, young O- or Be-type star, with clear orbital modulation observed across multiple wavelengths [2]. These modulations indicate that the gamma-ray emission is likely powered by intra-binary interactions — such as collisions between a relativistic outflow from the compact object and the dense stellar wind or radiation field of the companion star. TeV emission was detected from these compact systems, but it is unclear about the maximal energy reached by binary systems and whether they are capable of accelerating protons to PeV energies. Probing these systems at ultra-high-energy (UHE;  $>100$

---

\* E-mail: [dongxuqiang@ihp.ac.cn](mailto:dongxuqiang@ihp.ac.cn); [gmxiang@ihp.ac.cn](mailto:gmxiang@ihp.ac.cn); [licong@ihp.ac.cn](mailto:licong@ihp.ac.cn); [zjn@shao.ac.cn](mailto:zjn@shao.ac.cn); [hjh@ihp.ac.cn](mailto:hjh@ihp.ac.cn)

TeV) gamma-rays may open a unique window to study extreme particle acceleration, relativistic outflows, and the accretion–ejection processes operating in compact binary environments.

LS I +61° 303 is a prototypical gamma-ray binary system composed of a massive Be-type star and a compact object of uncertain nature [5, 6]. Recent reports of transient radio pulsations from the direction of LS I +61° 303 strongly suggest that the compact object is a rotating neutron star [7]. Located at a distance of  $\sim 2$  kiloparsecs [8], LS I +61° 303 exhibits a well-established orbital period of 26.496(8) days [9], confirmed across optical [10], X-ray [11, 12], and gamma-ray [13] bands. In 2006, the MAGIC telescope detected variable TeV gamma-ray emission modulated by the orbital period, with the short variability time scale suggesting a compact emission origin [14]. This orbital modulation was subsequently confirmed by VERITAS [15]. Both instruments detected enhanced TeV emission near apastron.

The Large High Altitude Air Shower Observatory (LHAASO) is a large hybrid observatory designed to explore the gamma-ray sky from  $\sim 100$  GeV to several PeV [16]. It consists of three major detector arrays: the Kilometer Square Array (KM2A), the Water Cherenkov Detector Array (WCDA) and the Wide Field-of-View Cherenkov Telescope Array (WFCTA) [17–19]. In this paper, we present LHAASO observations of LS I +61° 303, spanning roughly 1 TeV to several hundred TeV. These results provide unprecedented access to the ultra-high-energy regime and offer new constraints on the nature of particle acceleration in gamma-ray binaries.

## II. METHODS

Data from both WCDA and KM2A are used in this analysis. The WCDA data are collected with the full array from March 2021 to July 2024, and the number of triggered detectors ( $N_{\text{hit}}$ ) serves as a proxy for energy binning. The pininess parameter is used to separate gamma-rays from the cosmic ray background. The residual cosmic ray background after  $\gamma$ /hadron separation is estimated using the “direct integration method”.

The KM2A data used here are collected from December 2019 to July 2024, yielding an effective exposure of 1570.4 days after selection. The event-reconstruction algorithm and selection criteria are detailed in the performance paper [19]. The data are binned into five bins per energy decade based on the reconstructed energy, and the cosmic-ray background is estimated with the “direct integration method”.

A 3D likelihood fitting process is used to determine the spectrum and morphology simultaneously. The likelihood ratio test compares the goodness of fit between hypotheses. The test statistic is defined as  $\text{TS} = 2 \ln(\lambda)$ , with  $\lambda = \mathcal{L}_{s+b}/\mathcal{L}_b$ , where  $\mathcal{L}_{s+b}$  is the maximum likelihood for the source-plus-background model and  $\mathcal{L}_b$  is that for the background-only model. Following Wilks’s theorem [20], TS is converted to significance: under the null hypothesis TS follows a  $\chi^2$  distribution whose degrees of freedom equal the difference of free parameters between the background-only and source-plus-background models.

The sky map in celestial coordinates is divided into  $0.1^\circ \times 0.1^\circ$  pixels. The TS value at each pixel is obtained by the same likelihood fitting method. Specifically, we assume a point source template with a spectral index of -2.6 for WCDA and -3.0 for KM2A at every pixel; these indices reflect the typical spectra observed by each array.

To maintain consistent detector performance, only data taken with the full array from July 2021 to July 2024 are used for the orbital-variability analysis. The orbital phase of each event is calculated as  $\phi = ((T - T_0) \bmod P)/P$ , where  $T_0 = \text{MJD } 43366.275$  is the zero phase epoch [21],  $P = 26.496 \text{ d}$  is the orbital period [9], and  $\bmod$  denotes the modulo operator. We adopt the widely accepted periastron phase  $\phi_{\text{peri}} = 0.23$  [22, 23], although some alternative orbital solutions yield a slightly later phase ( $\phi_{\text{peri}} = 0.275$ ; [24]). The data are divided into ten phase bins per orbit. A likelihood-ratio test is employed: the null hypothesis assumes constant flux in all bins, whereas the alternative hypothesis allows the flux to vary among bins. Under Wilks’s theorem, the resulting TS follows a  $\chi^2$  distribution with 9 degrees of freedoms.

## III. RESULTS

Fig.1 shows the significance maps around LS I +61° 303 at two different energies. Concretely, the detection is at a significance level of  $9.2\sigma$  for WCDA and  $6.2\sigma$  for KM2A. With energy above 100 TeV, a total of 16 photon-like events are detected from the direction of LS I +61° 303 against a cosmic-ray background level of 5.1 events, corresponding to a significance of  $3.8\sigma$  according to the Li-Ma formula [27]. The total contribution from the nearest bright source, which is about  $1.9^\circ$  away from LS I +61° 303, as well as the Galactic diffuse emission, is estimated to be 0.12 events. The highest energy photon-like event, with the energy estimated to be  $267 \pm 75 \text{ TeV}$ , is detected at an angular distance of  $0.09^\circ$  away from LS I +61° 303. We estimate the energy uncertainty based on the simulations of the instrument’s response. The best fit position for WCDA using a 2D Gaussian model is  $\text{R.A.} = 40.10^\circ \pm 0.07_{\text{stat}}^\circ \pm 0.09_{\text{sys}}^\circ$  and  $\text{Decl.} = 61.33^\circ \pm 0.04_{\text{stat}}^\circ \pm 0.03_{\text{sys}}^\circ$ , while for KM2A it is  $\text{R.A.} = 40.18^\circ \pm 0.10_{\text{stat}}^\circ \pm 0.05_{\text{sys}}^\circ$  and  $\text{Decl.} = 61.16^\circ \pm 0.05_{\text{stat}}^\circ \pm 0.04_{\text{sys}}^\circ$ . The pointing accuracy is calibrated using similar zenith angle events (see the methods for detail). No significant

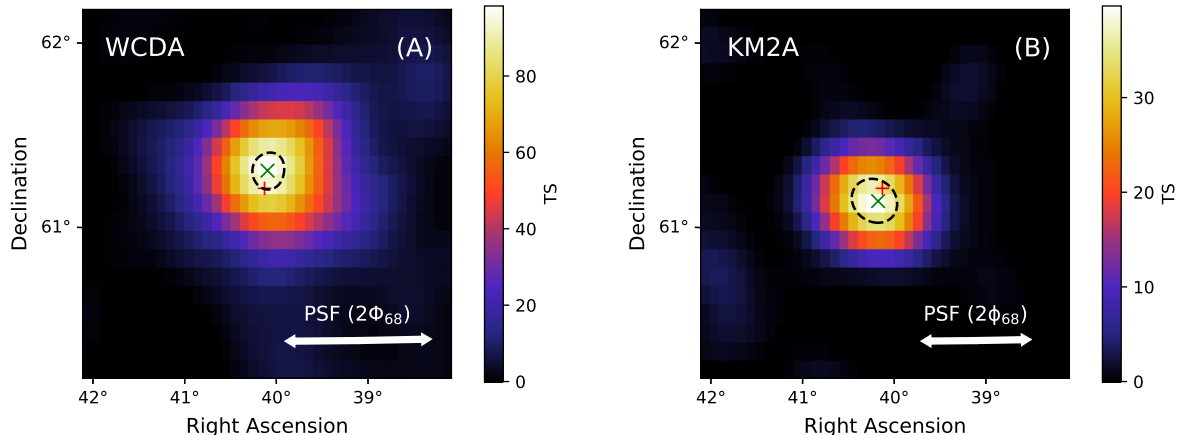


FIG. 1. Test-statistic maps after subtraction of the contributions from nearby sources and Galactic diffuse emission around LS I +61° 303, observed with WCDA (A) and KM2A (B), for the energy ranges 1.5–30.5 TeV and >25 TeV, respectively. Red crosses indicate the position of LS I +61° 303 at optical band [25], while the green ‘x’ represent the position of LS I +61° 303 as detected by LHAASO. The black dashed line indicates the positional uncertainty of LS I +61° 303 at the 95% level, which is consistent with the position measurement at X-ray band. PSF at each energy band is marked by double-headed arrow.

extension is detected; the 95% confidence level upper limits on extension width are 0.22° for WCDA and 0.25° for KM2A.

The gamma-ray spectrum shown in Fig. 2 can be described ( $\chi^2/ndf = 6.7/8$ ) by a single power law model  $dN/dE = N_0 \times (E/10\text{TeV})^{-\Gamma}$ , where  $N_0 = (2.18 \pm 0.20) \times 10^{-15} \text{ TeV}^{-1} \text{ cm}^{-2} \text{ s}^{-1}$  is the flux normalization and  $\Gamma = 3.00 \pm 0.05$  is the photon index. The integral flux above 1 TeV,  $F_{>1\text{TeV}} = 1.10 \times 10^{-12} \text{ cm}^{-2} \text{ s}^{-1}$ , corresponds to 3.8% of the Crab unit. The quoted errors are statistical only. Systematic uncertainties are assessed separately for WCDA and KM2A using the Crab Nebula as a standard candle, yielding  $^{+8}_{-24}\%$  and  $\pm 7\%$  for flux measurements, respectively. The difference between the atmospheric model used in the simulation and the actual atmosphere dominates the systematic error for KM2A; this introduces an uncertainty of 0.02 in the spectral index. Fig. 2 also shows the spectra measured by VERITAS and MAGIC for comparison. Although the flux of this source shows obvious orbital modulation, and the orbitally-averaged flux has shown slight changes on long time-scales (i.e. super-orbital modulation; [23, 28]), the TeV gamma-ray flux here is roughly consistent with those measured by MAGIC [14, 29] and VERITAS [26].

Benefiting from the broad energy coverage of LHAASO, we can probe the orbital modulation at different energy bands. From Fig. 3 we can see the phase-resolved flux measured by WCDA at 1.5–30.5 TeV, the emission extends over most phases and peaks near  $\phi = 0.6$ . A constant-flux hypothesis is rejected with  $p = 0.0053$  ( $\sim 2.8\sigma$ ). Between 25 and 100 TeV the emission is confined to  $\phi = 0.3 - 0.6$ , with  $p = 4.65 \times 10^{-5}$  ( $\sim 4.1\sigma$ ). Above 100 TeV the statistics are limited; we therefore split the data into two phase bins, 0.2–0.6 and 0.6–0.2, and find  $2.6\sigma$  evidence for modulation. Interestingly, the UHE photons cluster in the 0.6–0.2 phase range, differing from the distribution at low-energies. However, the significance is still too low for a firm conclusion.

#### IV. DISCUSSION AND CONCLUSION

In this study, we report the first definite detection of gamma-ray emission up to UHE range from the gamma-ray binary LS I +61° 303 using LHAASO observations. The extension of the spectral energy distribution to energies nearly an order of magnitude higher than previous measurements (e.g., by MAGIC and VERITAS) not only challenges conventional acceleration models but also provides a unique opportunity to probe the balance between particle acceleration and energy losses in such systems.

In the leptonic scenario, high-energy electrons upscatter stellar photons via inverse Compton (IC) scattering. However, in the UHE regime, where the IC scattering enters the Klein–Nishina regime (For a 100 TeV electron,  $\gamma\varepsilon \gg m_e c^2$  with  $\varepsilon = 1.9 \text{ eV}$ , corresponding to a Be-star temperature of 22.5 kK [30]), the IC process will be largely

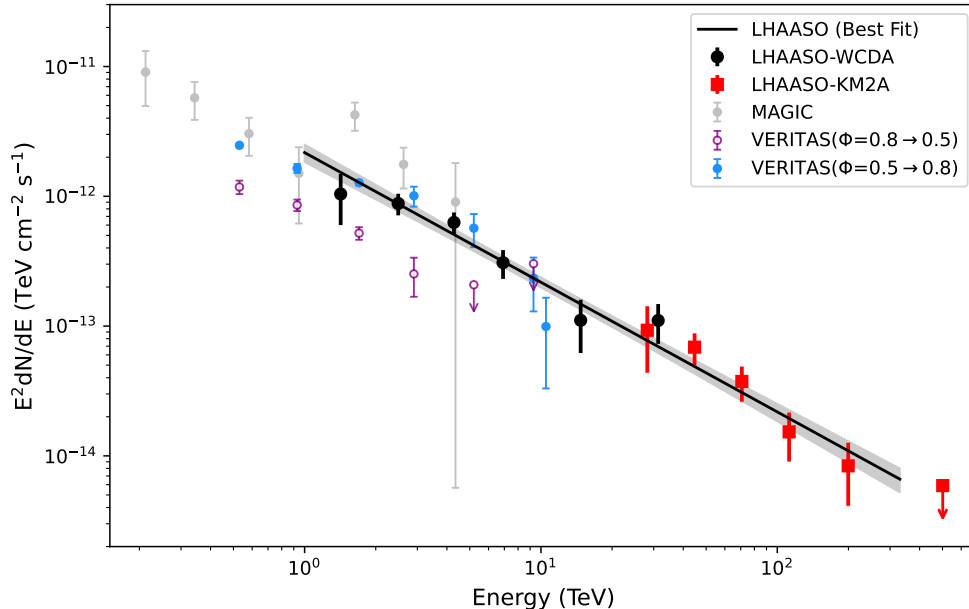


FIG. 2. Spectral energy distribution of LS I +61° 303 observed by LHAASO. The measurements from WCDA and KM2A are marked with black dots and red squares, respectively. The solid line represents the best-fit result assuming a power-law distribution, while the butterfly plot shows the  $1\sigma$  statistical uncertainties. For comparison, measurements from MAGIC (marked with gray points; [14]) and VERITAS (marked with purple circles for orbital phases from 0.8 to 0.5, and blue points for orbital phases from 0.5 to 0.8; [26]) are shown.

depressed. The IC process is also constrained by the maximum energy of electrons can be accelerated in binary systems, which is fundamentally determined by the the particle acceleration efficiency, cooling time and the limited size. Early studies [31, 32] have shown that the maximum energy is sensitive to parameters such as the magnetic field strength, the efficiency of the acceleration mechanism, and the ambient photon density. Assuming an acceleration timescale  $\tau_{\text{acc}} = E/(\eta e B c) \approx 1.1(E/1\text{TeV})(\eta/0.1)^{-1}(B/1\text{G})^{-1}$  s with efficiency factor  $\eta \approx 0.1$  and a magnetic field  $B \approx 0.2$  G [33], and a synchrotron cooling timescale  $t_{\text{syn}} = 6\pi m_e^2 c^3/(\sigma_T B^2 E) \approx 400(E/1\text{TeV})^{-1}(B/1\text{G})^{-2}$  s, the maximum energy  $E_{\text{max}}$  can be obtained by equating  $\tau_{\text{acc}}$  to the synchrotron cooling timescale  $t_{\text{syn}}$ , then  $E_{\text{max}} = \sqrt{6\pi\eta m_e^2 c^4/(\sigma_T B)} \approx 40$  TeV. Even if the acceleration efficiency is at its extreme maximum  $\eta = 1$  (Bohm diffusion limit), the attainable energy is only 130 TeV. Local magnetic field strength  $B(\phi)$  varies substantially along the orbit—due to changing orbital separation, shock compression, Be-disk crossings, and magnetic reconnection/turbulent amplification—so adopting an orbit-averaged  $B \approx 0.2$  G [33] may significantly misestimate the local  $E_{\text{max}}$ . Consequently, despite the detection of photons up to  $>200$  TeV, a purely leptonic scenario cannot yet be ruled out.

Hadronic processes are expected to be most efficient near periastron, as indicated by the flux enhancement around this orbital phase observed by KM2A. At these phases, the compact object encounters higher ambient densities, for instance through interaction with the circumstellar disk (possibly at its outer edge). Adopting the currently accepted orbital parameters of LS I +61° 303 (orbital period  $P \approx 26.5$  days, eccentricity  $e \approx 0.54$ , total mass  $M_{\text{tot}} \approx 14M_{\odot}$  [24] and then semi-major axis  $a \approx 0.4$  au), the radial density profile of the stellar wind can be expressed as  $n(r) = \dot{M}/(4\pi r^2 v_w m_p)$ , where we adopt canonical values for the mass-loss rate and velocity,  $\dot{M} \sim 5 \times 10^{-8} M_{\odot} \text{ yr}^{-1}$  and  $v_w = 10^8$  cm s $^{-1}$ . At periastron ( $r = r_p$ ), this yields  $n(r_p) \approx 1.9 \times 10^8$  cm $^{-3}$ . Within the Be-star disk, however, densities are 2–4 orders of magnitude higher; we adopt  $n_{\text{disk}} \sim 10^{11}$  cm $^{-3}$  as a fiducial value. The proton–proton cooling timescale is  $t_{pp} = (n\kappa_{pp}\sigma_{pp}c)^{-1}$ , with  $\sigma_{pp} \approx 40$  mbarn and  $\kappa_{pp} \approx 0.5$ . In the absence of disk-crossing events, one obtains  $t_{pp} \sim 100$  days, which is much longer than the orbital period and thus renders this scenario unlikely, whereas during disk crossing  $t_{pp} \sim 4.6$  hours. The interaction efficiency can be estimated as  $f_{pp} = t_{\text{esc}}/(t_{pp} + t_{\text{esc}})$ , where the escape/advection time is given by  $t_{\text{esc}} \sim l/v$ , with  $l \sim 10^{12}$  cm for a compact interaction zone and  $v \sim 10^9$  cm s $^{-1}$ , leading to  $t_{\text{esc}} \sim 10^3$  s. Consequently,  $f_{pp} \approx 0.08$  during disk-crossing episodes and  $f_{pp} \approx 1 \times 10^{-4}$  otherwise. Since only about one third of the pion energy is transferred into  $\pi^0 \rightarrow \gamma\gamma$ , the gamma-ray luminosity is related to the proton power by  $L_{\gamma} \approx f_{pp} L_p/3$ . From the KM2A spectrum, we infer a flux of  $F_{\gamma,25-100\text{TeV}} = 1.05 \times 10^{-13}$  erg cm $^{-2}$  s $^{-1}$ . Adopting a source distance of  $d \approx 2.0$  kpc, this corresponds to a gamma-ray luminosity of  $L_{\gamma} \approx 5 \times 10^{31}$  erg s $^{-1}$ .

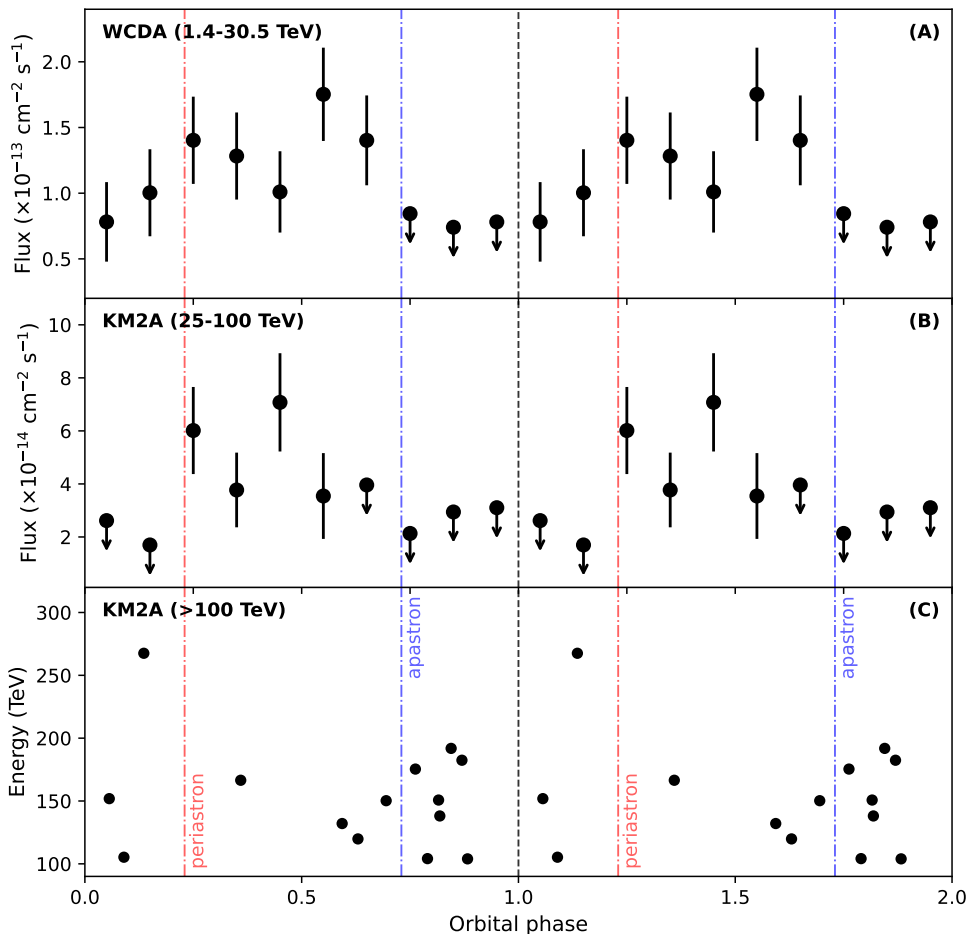


FIG. 3. (A,B) Flux measured by WCDA (1.4–30.5 TeV) and KM2A (25–100 TeV) versus orbital phase. (C) Energy of photons  $> 100$  TeV measured by KM2A versus orbital phase. Two orbital cycles are shown for clarity.

The required proton power is therefore  $L_p \approx 3L_\gamma/f_{pp}$ . During disk-crossing phases, this yields  $L_p \approx 1.9 \times 10^{33}$  erg  $s^{-1}$ , which is compatible with the spin-down power of a putative pulsar (assuming a pulsar with  $P \simeq 270$  ms [7], moment of inertia  $I \approx 10^{45}$  g  $cm^2$ , and period derivative  $\dot{P} = 3 \times 10^{-15}$  s  $s^{-1}$ , the spin-down luminosity is  $\dot{E} = 4\pi^2 I \dot{P} / P^3 \approx 6 \times 10^{33}$  erg  $s^{-1}$ ). Conversely, in the non-crossing scenario one obtains  $L_p \approx 1.5 \times 10^{36}$  erg  $s^{-1}$ , which significantly exceeds the available spin-down power.

Although the observed energy-dependent orbital modulation is only moderately significant, it nevertheless offers valuable insights into the physical conditions across the orbit. As discussed above, the flux enhancement observed by KM2A near periastron may originate from hadronic processes. In the WCDA energy band, however, the flux peak occurs at  $\phi \sim 0.6$  (consistent with the VERITAS results), but the light curve exhibits a more complex profile, suggesting the presence of multiple gamma-ray production mechanisms. A hint of UHE-photon concentration around apastron further supports a mixed two-zone scenario. In principle, electrons can be accelerated beyond 100 TeV if the acceleration site is slightly displaced from the binary system. Nevertheless, even if an extended outer accelerator (the Coriolis-induced termination shock [34]) is present at all orbital phases, its ability to produce observable  $> 100$  TeV photons may still be phase-dependent: near periastron the outer shock may be pushed inward and/or compressed by the stronger ram pressure, which can amplify the local magnetic field and shorten synchrotron loss times, thereby reducing the synchrotron-limited electron maximum energy; additionally, the higher local photon and matter densities increase  $\gamma\gamma$  opacity and promote electromagnetic cascades that reprocess ultra-high-energy photons to lower energies. By contrast, toward apastron the outer shock is expected to be more extended and less affected by strong radiative

losses, favoring acceleration and escape of electrons up to tens or hundreds of TeV and thus enhancing the visibility of  $>100$  TeV photons. Given the low statistics in the  $>100$  TeV band, these qualitative effects suffice to reconcile the apparent concentration of the handful of ultra-high-energy events at larger separations, while detailed quantitative modeling must await higher-significance data. Future observations with LHAASO, augmented by coordinated multi-wavelength campaigns, will provide a more comprehensive dataset: phase-resolved spectroscopy at the highest energies, deeper searches for  $>100$  TeV photons, and contemporaneous X-ray and radio monitoring (to track synchrotron cooling and shock activity) will be particularly valuable. Combined phase-resolved radiative-transfer and cascade modeling, constrained by these multi-band data, should be able to quantify the relative roles of inner/outer accelerators and test the scenario outlined above.

**Acknowledgements** We would like to thank all staff members who work at the LHAASO site above 4400 meters above sea level year round to maintain the detector and keep the water recycling system, electricity power supply and other components of the experiment operating smoothly. We are grateful to the Chengdu Management Committee of Tianfu New Area for the constant financial support for research with LHAASO data. We appreciate the computing and data service support provided by the National High Energy Physics Data Center for the data analysis in this paper. This research work is supported by the following grants: The National Natural Science Foundation of China(NSFC) No.12522510, No.12393851, No.12393852, No.12393853, No.12393854, No.12205314, No.12105301, No.12305120, No.12261160362, No.12105294, No.U1931201, No.12375107, No.12273038, CAS Project for Young Scientists in Basic Research(No. YSBR-061), Youth Innovation Promotion Association CAS(No.2022010, No.2023275) and in Thailand by the National Science and Technology Development Agency (NSTDA) and the National Research Council of Thailand (NRCT) under the High-Potential Research Team Grant Program (N42A650868).

## Appendix A: LHAASO detectors

The Large High Altitude Air Shower Observatory (LHAASO) is situated on Haizi Mountain in Daocheng County, Sichuan Province of China, standing at an altitude of 4,410 meters above sea level. It is a composite extensive air shower (EAS) detector array consisting of three sub-arrays: the Kilometer Square Array (KM2A), the 78,000 m Water Cherenkov Detector Array (WCDA), and the Wide Field-of-view atmospheric Cherenkov Telescope Array (WFCTA). The gamma rays for a wide energy range spanning from hundreds of GeV to several PeV are detected by WCDA and KM2A.

The data with energy above 25 TeV collected by KM2A are used in this analysis. KM2A comprises 5,216 electromagnetic particle detectors (EDs) and 1,188 underground muon detectors (MDs) spread over an area of approximately 1.3 km<sup>2</sup> [35]. The KM2A was incrementally developed and began operations, with half of the array starting scientific observations at the end of 2019, three-quarters operational by December 2020, and full operations officially launched on July 31, 2024, with a total exposure time of 1570.42 days. The ratio of measured muons to electrons is utilized to discriminate primary  $\gamma$ -rays from cosmic nuclei. Energies are estimated based on particle density at a radius of 50 m (denoted as  $\rho_{50}$ ) across various zenith angles [19]. The energy resolution is better than 20% for energies above 100 TeV within the zenith angle range of 0° – 35°. The data sets are categorized into five groups per decade based on reconstructed energy. The sky map is represented in celestial coordinates, divided into a grid of 0.1° × 0.1° pixels, with each pixel filled with the number of detected events corresponding to their reconstructed arrival direction. The “direct integration method” is employed to estimate the cosmic ray background. To optimize array performance, several event selection criteria are implemented. The data selection criteria used in this study align with the guidelines established in the publication by the collaboration in the Chinese Physics C (CPC) journal in 2021 [19].

The VHE data (0.8 TeV <  $E$  < 31 TeV) were collected by the whole WCDA. The data used in this study were obtained from the full-array operation of the WCDA from March 5, 2021, to July 31, 2024, with a total exposure time of 1124 days. The zenith angle of the shower was required to be less than 50 degrees. The Gamma/Proton separation parameter  $\mathcal{P}_{\text{inccness}}$  [36], is required to be less than 1.12, 1.02, 0.90, 0.88, 0.88, 0.84, and 0.84 for segments with  $N_{\text{hit}}$  value of [30–60],[60–100), [100–200), [200–300), [300–500), [500–800) and [800–2000]. For each  $N_{\text{hit}}$  segment, the sky map in celestial coordinates (right ascension and declination) was divided into a grid of 0.1° × 0.1°, which was filled with the number of the detected events according to their reconstructed arrival direction. The “direct integration method” [37] is adopted to estimate the number of CR background events in each pixel.

TABLE I. Energy bin definitions for WCDA (upper) and KM2A (lower) and the characteristics of LS I +61° 303 at each energy bin. Note that the definitions for WCDA and KM2A are different: WCDA data is binned depending on the number of triggered detector units( $N_{\text{hit}}$ ), and KM2A data is divided by the reconstructed energy.

$N_{\text{hit}}$	Median energy (TeV)	Differential Flux ( $\text{TeV}^{-1}\text{cm}^{-2}\text{s}^{-1}$ )	TS
30-60	0.83	$< 3.95 \times 10^{-12}$ (95% UL)	0.7
60-100	1.41	$(5.23 \pm 2.21) \times 10^{-13}$	5.6
100-200	2.49	$(1.42 \pm 0.27) \times 10^{-13}$	28.5
200-300	4.29	$(3.42 \pm 0.66) \times 10^{-14}$	28.9
300-500	6.91	$(6.45 \pm 1.61) \times 10^{-15}$	18.3
500-800	14.72	$(5.12 \pm 2.26) \times 10^{-16}$	6.7
800-2000	31.33	$(1.12 \pm 0.37) \times 10^{-16}$	14.4
$\log_{10}(E_{\text{rec}})$	Median energy (TeV)	Differential Flux ( $\text{TeV}^{-1}\text{cm}^{-2}\text{s}^{-1}$ )	TS
1.4-1.6	28.18	$(1.17 \pm 0.62) \times 10^{-16}$	4.0
1.6-1.8	44.67	$(3.45 \pm 0.96) \times 10^{-17}$	17.5
1.8-2.0	70.79	$(7.47 \pm 2.26) \times 10^{-18}$	13.8
2.0-2.2	112.20	$(1.22 \pm 0.50) \times 10^{-18}$	8.9
2.2-2.4	199.53	$(2.10 \pm 1.07) \times 10^{-19}$	6.6
2.4-3.0	501.19	$< 2.35 \times 10^{-20}$ (95% UL)	1.9

## Appendix B: Data analysis

Considering the influence from Galactic diffuse  $\gamma$ -ray emission (GDE) and nearby bright sources on LS I +61° 303, we define a 4°-radius circular ROI around LS I +61° 303, centered at R.A. = 40.1°, Decl. = 61.2° (see Fig. 4). The

only significant source inside this region is J0248+6021, which lies close to LS I +61° 303.

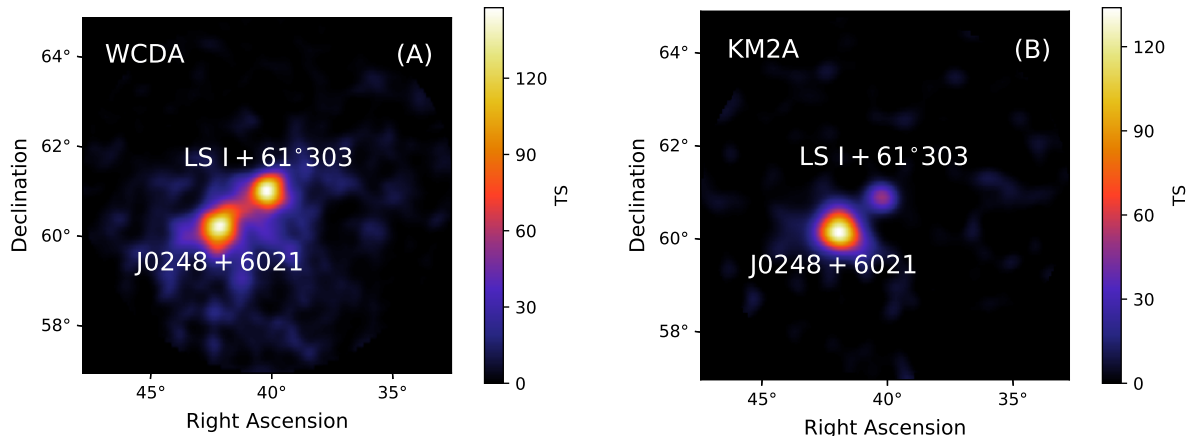


FIG. 4. Observed maps within ROI from WCDA (A) and KM2A (B).

We apply the 3D-likelihood method to analyze the dataset. The test statistic  $\Delta TS$  for LS I +61° 303 is 51.8 in the KM2A energy range, corresponding to a significance of  $6.2\sigma$ . We also fit the data with a power-law model with an exponential cutoff to test for potential curvature in the SED of LS I +61° 303. Compared to the pure power-law fit, the TS increases by 2 with one additional parameter. We therefore conclude that the pure power-law model is favored and no significant excess is observed in the SED. For WCDA, the SED is well described by a power law. Details of the median energy, flux, and TS in each energy bin for WCDA and KM2A are given in Table I.

Figure 5 shows the residual map after subtracting all sources within the ROI. No significant excess is visible in this map. The distribution of TS values is converted into statistical significance using Wilks's theorem and is well fit by a Gaussian. For WCDA the fit yields a mean of  $-0.055 \pm 0.010$  and a standard deviation of  $0.978 \pm 0.006$ . For KM2A we obtain a mean of  $0.033 \pm 0.007$  and a standard deviation of  $0.996 \pm 0.005$ .

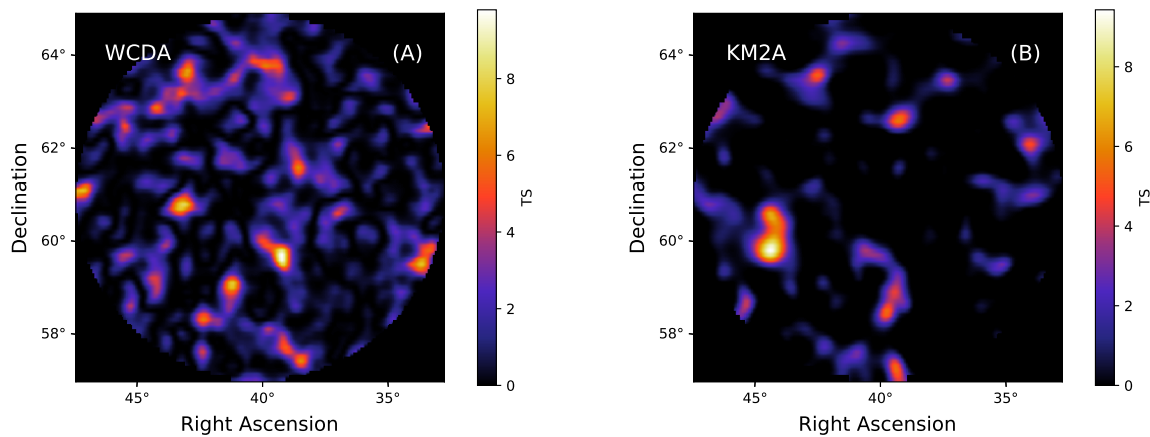


FIG. 5. 2D residual map from WCDA (A) and KM2A (B).

To evaluate the pointing error at the declination of LS I +61° 303, we've analysed Crab's position using events with zenith angle  $>30^\circ$  and adjusted the distribution of zenith angle to the path of LS I +61° 303. For KM2A, the largest deviation is  $0.036^\circ \pm 0.015^\circ$  in RA and  $0.028^\circ \pm 0.016^\circ$  in DEC. The pointing error of WCDA is calibrated using extra-galactic source 1ES 1959+650, which is at similar declination of LS I +61° 303. The deviation in RA and DEC are  $0.029 \pm 0.062$  and  $0.009 \pm 0.024$ . It should be noted that the deviation is dominated by statistics, and the pointing accuracy is calibrated to be better than  $0.03^\circ$  using all the events from Crab.

- 
- [1] H.-J. Grimm, M. Gilfanov, and R. Sunyaev, *Astronomy; Astrophysics* **391**, 923–944 (2002).
- [2] G. Dubus, *The Astronomy and Astrophysics Review* **21**, 10.1007/s00159-013-0064-5 (2013).
- [3] M. Chernyakova, D. Malyshev, A. Paizis, N. La Palombara, M. Balbo, R. Walter, B. Hnatyk, B. van Soelen, P. Romano, P. Munar-Adrover, I. Vovk, G. Piano, F. Capitanio, D. Falceta-Gonçalves, M. Landoni, P. L. Luque-Escamilla, J. Martí, J. M. Paredes, M. Ribó, S. Safi-Harb, L. Saha, L. Sidoli, and S. Vercellone, *aap* **631**, A177 (2019), [arXiv:1909.11018 \[astro-ph.HE\]](#).
- [4] M. Chernyakova and D. Malyshev, in *Multifrequency Behaviour of High Energy Cosmic Sources - XIII. 3-8 June 2019. Palermo* (2020) p. 45, [arXiv:2006.03615 \[astro-ph.HE\]](#).
- [5] J. M. Paredes, P. Marziani, J. Martí, J. Fabregat, M. J. Coe, C. Everall, F. Figueras, C. Jordi, A. J. Norton, T. Prince, V. Reglero, P. Roche, J. Torra, S. J. Unger, and R. Zamanov, *aap* **288**, 519 (1994), [arXiv:astro-ph/9402016 \[astro-ph\]](#).
- [6] P. C. Gregory and C. Neish, *The Astrophysical Journal* **580**, 1133 (2002).
- [7] S.-S. Weng *et al.*, *Nature Astron.* **6**, 698 (2022), [arXiv:2203.09423 \[astro-ph.HE\]](#).
- [8] I. A. Steele, I. Negueruela, M. J. Coe, and P. Roche, *mnras* **297**, L5 (1998), [arXiv:astro-ph/9803113 \[astro-ph\]](#).
- [9] A. R. Taylor and P. C. Gregory, *apj* **283**, 273 (1984).
- [10] H. Mendelson and T. Mazeh, *mnras* **239**, 733 (1989).
- [11] A. M. Levine and R. Corbet, *The Astronomer's Telegram* **940**, 1 (2006).
- [12] J. Li, D. F. Torres, and S. Zhang, *Astrophys. J. Lett.* **785**, L19 (2014), [arXiv:1402.6159 \[astro-ph.HE\]](#).
- [13] A. A. Abdo, M. Ackermann, M. Ajello, W. B. Atwood, M. Axelsson, L. Baldini, J. Ballet, G. Barbiellini, D. Bastieri, B. M. Baughman, K. Bechtol, R. Bellazzini, B. Berenji, R. Blandford, E. D. Bloom, E. Bonamente, A. W. Borgland, J. Bregeon, A. Brez, M. Brigida, P. Bruel, T. H. Burnett, G. A. Caliandro, R. A. Cameron, P. A. Caraveo, J. M. Casandjian, E. Cavazzuti, C. Cecchi, Ö. Çelik, E. Charles, S. Chaty, A. Chekhtman, C. C. Cheung, J. Chiang, S. Ciprini, R. Claus, J. Cohen-Tanugi, L. R. Cominsky, J. Conrad, S. Corbel, R. Corbet, S. Cutini, C. D. Dermer, A. de Angelis, A. de Luca, F. de Palma, S. W. Digel, M. Dormody, E. do Couto e Silva, P. S. Drell, R. Dubois, G. Dubus, D. Dumora, C. Farnier, C. Favuzzi, S. J. Fegan, W. B. Focke, M. Frailis, Y. Fukazawa, S. Funk, P. Fusco, F. Gargano, D. Gasparrini, N. Gehrels, S. Germani, B. Giebels, N. Giglietto, F. Giordano, T. Glanzman, G. Godfrey, I. A. Grenier, M. H. Grondin, J. E. Grove, L. Guillemot, S. Guiriec, Y. Hanabata, A. K. Harding, M. Hayashida, E. Hays, A. B. Hill, R. E. Hughes, G. Jóhannesson, A. S. Johnson, R. P. Johnson, T. J. Johnson, W. N. Johnson, T. Kamae, H. Katagiri, J. Kataoka, N. Kawai, M. Kerr, J. Knödseder, M. L. Kocian, F. Kuehn, M. Kuss, J. Lande, S. Larsson, L. Latronico, F. Longo, F. Loparco, B. Lott, M. N. Lovellette, P. Lubrano, G. M. Madejski, A. Makeev, M. Marelli, M. N. Mazziotta, J. E. McEnery, C. Meurer, P. F. Michelson, W. Mitthumsiri, T. Mizuno, C. Monte, M. E. Monzani, A. Morselli, I. V. Moskalenko, S. Murgia, P. L. Nolan, E. Nuss, T. Ohsugi, A. Okumura, N. Omodei, E. Orlando, J. F. Ormes, D. Paneque, J. H. Panetta, D. Parent, V. Pelassa, M. Pepe, M. Pesce-Rollins, F. Piron, T. A. Porter, S. Rainò, R. Rando, P. S. Ray, M. Razzano, N. Rea, A. Reimer, O. Reimer, T. Reposeur, S. Ritz, L. S. Rochester, A. Y. Rodriguez, R. W. Romani, F. Ryde, H. F. W. Sadrozinski, D. Sanchez, A. Sander, P. M. Saz Parkinson, J. D. Scargle, C. Sgrò, M. S. Shaw, A. Sierpowska-Bartosik, E. J. Siskind, D. A. Smith, P. D. Smith, G. Spandre, P. Spinelli, E. Striani, M. S. Strickman, D. J. Suson, H. Tajima, H. Takahashi, T. Takahashi, T. Tanaka, J. B. Thayer, J. G. Thayer, D. J. Thompson, L. Tibaldo, D. F. Torres, G. Tosti, A. Tramacere, Y. Uchiyama, T. L. Usher, V. Vasileiou, N. Vilchez, V. Vitale, A. P. Waite, P. Wang, B. L. Winer, K. S. Wood, T. Ylinen, and M. Ziegler, *apjl* **701**, L123 (2009), [arXiv:0907.4307 \[astro-ph.HE\]](#).
- [14] J. Albert, E. Aliu, H. Anderhub, P. Antoranz, A. Armada, M. Asensio, C. Baixeras, J. A. Barrio, M. Bartelt, H. Bartko, D. Bastieri, S. R. Bavikadi, W. Bednarek, K. Berger, C. Bigongiari, A. Biland, E. Bisesi, R. K. Bock, P. Bordas, V. Bosch-Ramon, T. Bretz, I. Britvitch, M. Camara, E. Carmona, A. Chilingarian, S. Ciprini, J. A. Coarasa, S. Commichau, J. L. Contreras, J. Cortina, V. Curtef, V. Danielyan, F. Dazzi, A. De Angelis, R. de los Reyes, B. De Lotto, E. Domingo-Santamaría, D. Dorner, M. Doro, M. Errando, M. Fagiolini, D. Ferenc, E. Fernández, R. Firpo, J. Flix, M. V. Fonseca, L. Font, M. Fuchs, N. Galante, M. Garczarczyk, M. Gaug, M. Giller, F. Goebel, D. Hakobyan, M. Hayashida, T. Hengstebeck, D. Höhne, J. Hose, C. C. Hsu, P. G. Isar, P. Jacon, O. Kalekin, R. Kosyra, D. Kranich, M. Laatiaoui, A. Laille, T. Lenisa, P. Liebing, E. Lindfors, S. Lombardi, F. Longo, J. López, M. López, E. Lorenz, F. Lucarelli, P. Majumdar, G. Maneva, K. Mannheim, O. Mansutti, M. Mariotti, M. Martínez, K. Mase, D. Mazin, C. Merck, M. Meucci, M. Meyer, J. M. Miranda, R. Mirzoyan, S. Mizobuchi, A. Moralejo, K. Nilsson, E. Oña-Wilhelmi, R. Orduña, N. Otte, I. Oya, D. Paneque, R. Paoletti, J. M. Paredes, M. Pasanen, D. Pascoli, F. Pauss, N. Pavel, R. Pegna, M. Persic, L. Peruzzo, A. Piccioli, M. Poller, G. Pooley, E. Prandini, A. Raymers, W. Rhode, M. Ribó, J. Rico, B. Riegel, M. Rissi, A. Robert, G. E. Romero, S. Rügamer, A. Saggion, A. Sánchez, P. Sartori, V. Scalzotto, V. Scapin, R. Schmitt, T. Schweizer, M. Shayduk, K. Shinozaki, S. N. Shore, N. Sidro, A. Sillanpää, D. Sobczynska, A. Stamerra, L. S. Stark, L. Takalo, P. Temnikov, D. Tesaro, M. Teshima, N. Tonello, A. Torres, D. F. Torres, N. Turini, H. Vankov, V. Vitale, R. M. Wagner, T. Wibig,

- W. Wittek, R. Zanin, and J. Zapatero, *Science* **312**, 1771 (2006), [arXiv:astro-ph/0605549 \[astro-ph\]](#).
- [15] e. a. Acciari, *apj* **679**, 1427 (2008), [arXiv:0802.2363 \[astro-ph\]](#).
- [16] Z. Cao, D. della Volpe, S. Liu, Editors, ;, X. Bi, Y. Chen, B. D. Piazzoli, L. Feng, H. Jia, Z. Li, X. Ma, X. Wang, X. Zhang, E. Referees, ;, X. Qie, H. Hu, I. Referees, ;, A. Sáiz, R. Yang, Contributors, ;, A. Addazi, K. Belotsky, V. Beylin, Y.-J. Bi, M.-J. Che, S.-Z. Chen, Y.-D. Cheng, A. Chiavassa, M. Cirelli, G. D. Sciascio, A. Esmaili, K. Fang, N. Fornengo, Q. Gou, Y.-Q. Guo, Q. Gan, G.-H. Gong, M.-H. Gu, H. He, H.-H. He, C. Hou, X.-T. Huang, W.-H. Huang, M. Kachekriess, M. Khlopov, V. Korchagin, A. Korochkin, V. Kuksa, L. T. Ksenofontov, Y. Liu, R.-Y. Liu, C. Liu, A. Marciano, O. Martineau-Huynh, D. Martraire, L. Ma, A. Neronov, P. Panci, R. Pasechnik, D. Ruffolo, A. Sakharov, F. Sala, D. Semikoz, O. Shchegolev, P. D. Serpico, X.-D. Sheng, Y. V. Stenkin, P. H. T. Tam, S. Vernetto, P. Vallania, N. Volchanskiy, Z. Wang, K. Wang, X.-Y. Wang, H.-R. Wu, C.-Y. Wu, S. Wu, G. Xiao, R. zhi Yang, D. Yan, Z.-G. Yao, P. Yin, Q. Yuan, X. Zhang, H. Zeng, S.-S. Zhang, Y. Zhang, X. Zhou, H. Zhu, and X. Zuo, *The large high altitude air shower observatory (lhaaso) science book (2021 edition)* (2022), [arXiv:1905.02773 \[astro-ph.HE\]](#).
- [17] F. Aharonian *et al.* (LHAASO), *Chin. Phys. C* **45**, 085002 (2021).
- [18] Z. Cao, F. Aharonian, Q. An, , Y. Bai, Y. Bao, D. Bastieri, X. Bi, Y. Bi, J. Cai, Q. Cao, W. Cao, Z. Cao, J. Chang, J. Chang, A. Chen, E. Chen, L. Chen, L. Chen, L. Chen, M. Chen, M. Chen, Q. Chen, S. Chen, T. Chen, Y. Chen, N. Cheng, Y. Cheng, M. Cui, S. Cui, X. Cui, Y. Cui, B. Dai, H. Dai, Z. Dai, , D. della Volpe, X. Dong, K. Duan, J. Fan, Y. Fan, J. Fang, K. Fang, C. Feng, L. Feng, S. Feng, X. Feng, Y. Feng, S. Gabici, B. Gao, C. Gao, L. Gao, Q. Gao, W. Gao, W. Gao, M. Ge, L. Geng, G. Giacinti, G. Gong, Q. Gou, M. Gu, F. Guo, X. Guo, Y. Guo, Y. Guo, Y. Guo, Y. Han, H. He, H. He, J. He, X. He, Y. He, M. Heller, Y. Hor, B. Hou, C. Hou, X. Hou, H. Hu, Q. Hu, S. Hu, D. Huang, T. Huang, W. Huang, X. Huang, X. Huang, Y. Huang, Z. Huang, X. Ji, H. Jia, K. Jia, K. Jiang, X. Jiang, Z. Jiang, M. Jin, M. Kang, T. Ke, D. Kuleshov, K. Kurinov, B. Li, C. Li, C. Li, D. Li, F. Li, H. Li, H. Li, H. Li, J. Li, J. Li, J. Li, K. Li, W. Li, W. Li, X. Li, X. Li, Y. Li, Z. Li, Z. Li, E. Liang, Y. Liang, S. Lin, B. Liu, C. Liu, D. Liu, H. Liu, H. Liu, J. Liu, J. Liu, J. Liu, M. Liu, R. Liu, S. Liu, W. Liu, Y. Liu, Y. Liu, R. Lu, Q. Luo, H. Lv, B. Ma, L. Ma, X. Ma, J. Mao, Z. Min, W. Mitthumsiri, H. Mu, Y. Nan, A. Neronov, Z. Ou, B. Pang, P. Pattarakijwanich, Z. Pei, M. Qi, Y. Qi, B. Qiao, J. Qin, D. Ruffolo, A. Sáiz, D. Semikoz, C. Shao, L. Shao, O. Shchegolev, X. Sheng, F. Shu, H. Song, Y. Stenkin, V. Stepanov, Y. Su, Q. Sun, X. Sun, Z. Sun, P. Tam, Q. Tang, Z. Tang, W. Tian, C. Wang, C. Wang, G. Wang, H. Wang, H. Wang, J. Wang, K. Wang, L. Wang, L. Wang, P. Wang, R. Wang, W. Wang, X. Wang, X. Wang, Y. Wang, Y. Wang, Y. Wang, Z. Wang, Z. Wang, Z. Wang, Z. Wang, D. Wei, J. Wei, Y. Wei, T. Wen, C. Wu, H. Wu, S. Wu, X. Wu, Y. Wu, S. Xi, J. Xia, J. Xia, G. Xiang, D. Xiao, G. Xiao, G. Xin, Y. Xin, Y. Xing, Z. Xiong, D. Xu, R. Xu, R. Xu, W. Xu, L. Xue, D. Yan, J. Yan, T. Yan, C. Yang, F. Yang, F. Yang, H. Yang, J. Yang, L. Yang, M. Yang, R. Yang, S. Yang, Y. Yao, Z. Yao, Y. Ye, L. Yin, N. Yin, X. You, Z. You, Y. Yu, Q. Yuan, H. Yue, H. Zeng, T. Zeng, W. Zeng, M. Zha, B. Zhang, F. Zhang, H. Zhang, H. Zhang, J. Zhang, L. Zhang, L. Zhang, P. Zhang, P. Zhang, R. Zhang, S. Zhang, S. Zhang, S. Zhang, X. Zhang, X. Zhang, Y. Zhang, Y. Zhang, Y. Zhang, B. Zhao, J. Zhao, L. Zhao, L. Zhao, S. Zhao, F. Zheng, B. Zhou, H. Zhou, J. Zhou, M. Zhou, P. Zhou, R. Zhou, X. Zhou, C. Zhu, F. Zhu, H. Zhu, K. Zhu, X. Zuo, and L. Collaboration), *Chinese Physics C* **48**, 065001 (2024).
- [19] F. Aharonian, Q. An, Axikegu, L. X. Bai, Y. X. Bai, Y. W. Bao, D. Bastieri, X. J. Bi, Y. J. Bi, H. Cai, J. T. Cai, Z. Cao, Z. Cao, J. Chang, J. F. Chang, X. C. Chang, B. M. Chen, J. Chen, L. Chen, L. Chen, L. Chen, M. J. Chen, M. L. Chen, Q. H. Chen, S. H. Chen, S. Z. Chen, T. L. Chen, X. L. Chen, Y. Chen, N. Cheng, Y. D. Cheng, S. W. Cui, X. H. Cui, Y. D. Cui, B. Z. Dai, H. L. Dai, Z. G. Dai, Danzengluobu, D. della Volpe, B. D. Piazzoli, X. J. Dong, J. H. Fan, Y. Z. Fan, Z. X. Fan, J. Fang, K. Fang, C. F. Feng, L. Feng, S. H. Feng, Y. L. Feng, B. Gao, C. D. Gao, Q. Gao, W. Gao, M. M. Ge, L. S. Geng, G. H. Gong, Q. B. Gou, M. H. Gu, J. G. Guo, X. L. Guo, Y. Q. Guo, Y. Y. Guo, Y. A. Han, H. H. He, H. N. He, J. C. He, S. L. He, X. B. He, Y. He, M. Heller, Y. K. Hor, C. Hou, X. Hou, H. B. Hu, S. Hu, S. C. Hu, X. J. Hu, D. H. Huang, Q. L. Huang, W. H. Huang, X. T. Huang, Z. C. Huang, F. Ji, X. L. Ji, H. Y. Jia, K. Jiang, Z. J. Jiang, C. Jin, D. Kuleshov, K. Levochkin, B. B. Li, C. Li, C. Li, F. Li, H. B. Li, H. C. Li, H. Y. Li, J. Li, K. Li, W. L. Li, X. Li, X. Li, X. R. Li, Y. Li, Y. Z. Li, Z. Li, Z. Li, E. W. Liang, Y. F. Liang, S. J. Lin, B. Liu, C. Liu, D. Liu, H. Liu, H. D. Liu, J. Liu, J. L. Liu, J. S. Liu, J. Y. Liu, M. Y. Liu, R. Y. Liu, S. M. Liu, W. Liu, Y. N. Liu, Z. X. Liu, W. J. Long, R. Lu, H. K. Lv, B. Q. Ma, L. L. Ma, X. H. Ma, J. R. Mao, A. Masood, W. Mitthumsiri, T. Montaruli, Y. C. Nan, B. Y. Pang, P. Pattarakijwanich, Z. Y. Pei, M. Y. Qi, D. Ruffolo, V. Rulev, A. Sáiz, L. Shao, O. Shchegolev, X. D. Sheng, J. R. Shi, H. C. Song, Y. V. Stenkin, V. Stepanov, Q. N. Sun, X. N. Sun, Z. B. Sun, P. H. T. Tam, Z. B. Tang, W. W. Tian, B. D. Wang, C. Wang, H. Wang, H. G. Wang, J. C. Wang, J. S. Wang, L. P. Wang, L. Y. Wang, R. N. Wang, W. Wang, W. Wang, X. G. Wang, X. J. Wang, X. Y. Wang, Y. D. Wang, Y. J. Wang, Y. P. Wang, Z. Wang, Z. Wang, Z. H. Wang, Z. X. Wang, D. M. Wei, J. J. Wei, Y. J. Wei, T. Wen, C. Y. Wu, H. R. Wu, S. Wu, W. X. Wu, X. F. Wu, S. Q. Xi, J. Xia, J. J. Xia, G. M. Xiang, G. Xiao, H. B. Xiao, G. G. Xin, Y. L. Xin, Y. Xing, D. L. Xu, R. X. Xu, L. Xue, D. H. Yan, C. W. Yang, F. F. Yang, J. Y. Yang, L. L. Yang, M. J. Yang, R. Z. Yang, S. B. Yang, Y. H. Yao, Z. G. Yao, Y. M. Ye, L. Q. Yin, N. Yin, X. H. You, Z. Y. You, Y. H. Yu, Q. Yuan, H. D. Zeng, T. X. Zeng, W. Zeng, Z. K. Zeng, M. Zha, X. X. Zhai, B. B. Zhang, H. M. Zhang, H. Y. Zhang, J. L. Zhang, J. W. Zhang, L. Zhang, L. Zhang, L. X. Zhang, P. F. Zhang, P. P. Zhang, R. Zhang, S. R. Zhang, S. S. Zhang, X. Zhang, X. P. Zhang, Y. Zhang, Y. Zhang, Y. F. Zhang, Y. L. Zhang, B. Zhao, J. Zhao, L. Zhao, L. Z. Zhao, S. P. Zhao, F. Zheng, Y. Zheng, B. Zhou, H. Zhou, J. N. Zhou, P. Zhou, R. Zhou, X. X. Zhou, C. G. Zhu, F. R. Zhu, H. Zhu, K. J. Zhu, X. Zuo, and L. Collaboration), *Chinese Physics C* **45**, 025002 (2021).
- [20] S. S. Wilks, *The Annals of Mathematical Statistics* **9**, 60 (1938).
- [21] A. R. Taylor and P. C. Gregory, *apj* **255**, 210 (1982).
- [22] J. Casares, I. Ribas, J. M. Paredes, J. Martí, and C. Allende Prieto, *mnras* **360**, 1105 (2005), [arXiv:astro-ph/0504332 \[astro-ph\]](#).
- [23] M. L. Ahnen, S. Ansoldi, L. A. Antonelli, P. Antoranz, A. Babic, B. Banerjee, P. Bangale, U. Barres de Almeida, J. A.

- Barrio, J. Becerra González, W. Bednarek, E. Bernardini, B. Biasuzzi, A. Biland, O. Blanch, S. Bonnefoy, G. Bonnoli, F. Borracci, T. Bretz, S. Buson, A. Carosi, A. Chatterjee, R. Clavero, P. Colin, E. Colombo, J. L. Contreras, J. Cortina, S. Covino, P. Da Vela, F. Dazzi, A. De Angelis, B. De Lotto, E. de Oña Wilhelmi, C. Delgado Mendez, F. Di Pierro, A. Domínguez, D. Dominis Prester, D. Dorner, M. Doro, S. Einecke, D. Eisenacher Glawion, D. Elsaesser, A. Fernández-Barral, D. Fidalgo, M. V. Fonseca, L. Font, K. Frantzen, C. Fruck, D. Galindo, R. J. García López, M. Garczarczyk, D. Garrido Terrats, M. Gaug, P. Giammaria, N. Godinović, A. González Muñoz, D. Gora, D. Guberman, D. Hadasch, A. Hahn, Y. Hanabata, M. Hayashida, J. Herrera, J. Hose, D. Hrupec, G. Hughes, W. Idec, K. Kodani, Y. Konno, H. Kubo, J. Kushida, A. La Barbera, D. Lelas, E. Lindfors, S. Lombardi, F. Longo, M. López, R. López-Coto, A. López-Oramas, P. Majumdar, M. Makariev, K. Mallot, G. Maneva, M. Manganaro, K. Mannheim, L. Maraschi, B. Marcote, M. Mariotti, M. Martínez, D. Mazin, U. Menzel, J. M. Miranda, R. Mirzoyan, A. Moralejo, E. Moretti, D. Nakajima, V. Neustroev, A. Niedzwiecki, M. Nieves Rosillo, K. Nilsson, K. Nishijima, K. Noda, R. Orito, A. Overkemping, S. Paiano, J. Palacio, M. Palatiello, D. Paneque, R. Paoletti, J. M. Paredes, X. Paredes-Fortuny, G. Pedalletti, M. Persic, J. Poutanen, P. G. Prada Moroni, E. Prandini, I. Puljak, W. Rhode, M. Ribó, J. Rico, J. Rodríguez García, T. Saito, K. Satalecka, C. Schultz, T. Schweizer, S. N. Shore, A. Sillanpää, J. Sitarek, I. Snidaric, D. Sobczynska, A. Stamerra, T. Steinbring, M. Strzys, L. Takalo, H. Takami, F. Tavecchio, P. Temnikov, T. Terzić, D. Tescaro, M. Teshima, J. Thaele, D. F. Torres, T. Toyama, A. Treves, V. Verguilov, I. Vovk, J. E. Ward, M. Will, M. H. Wu, R. Zanin, MAGIC Collaboration, J. Casares, and A. Herrero, *aap* **591**, A76 (2016), [arXiv:1603.06973 \[astro-ph.HE\]](#).
- [24] C. Aragona, M. V. McSwain, E. D. Grundstrom, A. N. Marsh, R. M. Roettenbacher, K. M. Hessler, T. S. Boyajian, and P. S. Ray, *Astrophys. J.* **698**, 514 (2009), [arXiv:0902.4015 \[astro-ph.HE\]](#).
- [25] Gaia Collaboration, A. Vallenari, A. G. A. Brown, T. Prusti, J. H. J. de Bruijne, F. Arenou, C. Babusiaux, M. Biermann, O. L. Creevey, C. Ducourant, D. W. Evans, L. Eyer, R. Guerra, A. Hutton, C. Jordi, S. A. Klioner, U. L. Lammers, L. Lindegren, X. Luri, F. Mignard, C. Panem, D. Pourbaix, S. Randich, P. Sartoretti, C. Soubiran, P. Tanga, N. A. Walton, C. A. L. Bailer-Jones, U. Bastian, R. Drimmel, F. Jansen, D. Katz, M. G. Lattanzi, F. van Leeuwen, J. Bakker, C. Cacciari, J. Castañeda, F. De Angeli, C. Fabricius, M. Foesneanu, Y. Frémat, L. Galluccio, A. Guerrier, U. Heiter, E. Masana, R. Messineo, N. Mowlavi, C. Nicolas, K. Nienartowicz, F. Pailler, P. Panuzzo, F. Riclet, W. Roux, G. M. Seabroke, R. Sordo, F. Thévenin, G. Gracia-Abril, J. Portell, D. Teyssier, M. Altmann, R. Andrae, M. Audard, I. Bellas-Velidis, K. Benson, J. Berthier, R. Blomme, P. W. Burgess, D. Busonero, G. Busso, H. Cánovas, B. Carry, A. Cellino, N. Cheek, G. Clementini, Y. Damerdjji, M. Davidson, P. de Teodoro, M. Nuñez Campos, L. Delchambre, A. Dell’Oro, P. Esquej, J. Fernández-Hernández, E. Fraile, D. Garabato, P. García-Lario, E. Gosset, R. Haigron, J. L. Halbwegs, N. C. Hambly, D. L. Harrison, J. Hernández, D. Hestroffer, S. T. Hodgkin, B. Holl, K. Janßen, G. Jevardat de Fombelle, S. Jordan, A. Krone-Martins, A. C. Lanzafame, W. Löffler, O. Marchal, P. M. Marrese, A. Moitinho, K. Muinonen, P. Osborne, E. Pancino, T. Pauwels, A. Recio-Blanco, C. Reylé, M. Riello, L. Rimoldini, T. Roegiers, J. Rybizki, L. M. Sarro, C. Siopis, M. Smith, A. Sozzetti, E. Utrilla, M. van Leeuwen, U. Abbas, P. Ábrahám, A. Abreu Aramburu, C. Aerts, J. J. Aguado, M. Ajaj, F. Aldean-Montero, G. Altavilla, M. A. Álvarez, J. Alves, F. Anders, R. I. Anderson, E. Anglada Varela, T. Antoja, D. Baines, S. G. Baker, L. Balaguer-Núñez, E. Balbinot, Z. Balog, C. Barache, D. Barbato, M. Barros, M. A. Barstow, S. Bartolomé, J. L. Bassilana, N. Bauchet, U. Becciani, M. Bellazzini, A. Berihuete, M. Bernet, S. Bertone, L. Bianchi, A. Binnenfeld, S. Blanco-Cuaresma, A. Blazere, T. Boch, A. Bombrun, D. Bossini, S. Bouquillon, A. Bragaglia, L. Bramante, E. Breedt, A. Bressan, N. Brouillet, E. Brugaletta, B. Bucciarelli, A. Burlacu, A. G. Butkevich, R. Buzzzi, E. Caffau, R. Cancelliere, T. Cantat-Gaudin, R. Carballo, T. Carlucci, M. I. Carnerero, J. M. Carrasco, L. Casamiquela, M. Castellani, A. Castro-Ginard, L. Chaoul, P. Charlot, L. Chemin, V. Chiaramida, A. Chiavassa, N. Chornay, G. Comoretto, G. Contursi, W. J. Cooper, T. Cornez, S. Cowell, F. Crifo, M. Cropper, M. A. Crosta, C. Crowley, C. Daponte, A. Dapergolas, M. David, P. David, P. de Laverny, F. De Luise, and R. De March, *Astron. & Astrophys.* **674**, A1 (2023), [arXiv:2208.00211 \[astro-ph.GA\]](#).
- [26] P. Kar and VERITAS Collaboration, in *35th International Cosmic Ray Conference (ICRC2017)*, International Cosmic Ray Conference, Vol. 301 (2017) p. 712, [arXiv:1708.05107 \[astro-ph.HE\]](#).
- [27] T. P. Li and Y. Q. Ma, *Astrophys. J.* **272**, 317 (1983).
- [28] J. Li, D. F. Torres, S. Zhang, D. Hadasch, N. Rea, G. A. Calciandro, Y. Chen, and J. Wang, *Astrophys. J. Lett.* **744**, L13 (2012), [arXiv:1111.7068 \[astro-ph.HE\]](#).
- [29] J. Albert *et al.* (MAGIC), *Astrophys. J.* **693**, 303 (2009), [arXiv:0806.1865 \[astro-ph\]](#).
- [30] J. Martí and J. M. Paredes, *Astron. & Astrophys.* **298**, 151 (1995).
- [31] D. Khangulyan, S. Hnatic, F. Aharonian, and S. Bogovalov, *mnras* **380**, 320 (2007), [arXiv:astro-ph/0605663 \[astro-ph\]](#).
- [32] D. Khangulyan, F. Aharonian, and V. Bosch-Ramon, *mnras* **383**, 467 (2008), [arXiv:0707.1689 \[astro-ph\]](#).
- [33] V. Zabalza, J. M. Paredes, and V. Bosch-Ramon, *aap* **527**, A9 (2011), [arXiv:1011.4489 \[astro-ph.HE\]](#).
- [34] V. Zabalza, V. Bosch-Ramon, F. Aharonian, and D. Khangulyan, *aap* **551**, A17 (2013), [arXiv:1212.3222 \[astro-ph.HE\]](#).
- [35] H. He, *Radiation Detection Technology and Methods* **2** (2018).
- [36] A. U. Abeysekara, A. Albert, R. Alfaro, C. Alvarez, J. D. Álvarez, R. Arceo, J. C. Arteaga-Velázquez, H. A. Ayala Solares, A. S. Barber, N. Bautista-Elivar, A. Becerril, E. Belmont-Moreno, S. Y. BenZvi, D. Berley, J. Braun, C. Brisbois, K. S. Caballero-Mora, T. Capistrán, A. Carramiñana, S. Casanova, M. Castillo, U. Cotti, J. Cotzomi, S. Coutiño de León, E. de la Fuente, C. De León, T. DeYoung, B. L. Dingus, M. A. DuVernois, J. C. Díaz-Vélez, R. W. Ellsworth, D. W. Fiorino, N. Fraija, J. A. García-González, M. Gerhardt, A. González Muñoz, M. M. González, J. A. Goodman, Z. Hampel-Arias, J. P. Harding, S. Hernandez, A. Hernandez-Almada, J. Hinton, C. M. Hui, P. Hütemeyer, A. Iriarte, A. Jardin-Blicq, V. Joshi, S. Kaufmann, D. Kieda, A. Lara, R. J. Lauer, W. H. Lee, D. Lennarz, H. León Vargas, J. T. Linnemann, A. L. Longinotti, G. L. Raya, R. Luna-García, R. López-Coto, K. Malone, S. S. Marinelli, O. Martinez, I. Martinez-Castellanos, J. Martínez-Castro, H. Martínez-Huerta, J. A. Matthews, P. Miranda-Romagnoli, E. Moreno, M. Mostafá,

- L. Nellen, M. Newbold, M. U. Nisa, R. Noriega-Papaqui, R. Pelayo, J. Pretz, E. G. Pérez-Pérez, Z. Ren, C. D. Rho, C. Rivière, D. Rosa-González, M. Rosenberg, E. Ruiz-Velasco, H. Salazar, F. Salesa Greus, A. Sandoval, M. Schneider, H. Schoorlemmer, G. Sinnis, A. J. Smith, R. W. Springer, P. Surajbali, I. Taboada, O. Tibolla, K. Tollefson, I. Torres, T. N. Ukwatta, L. Villaseñor, T. Weisgarber, S. Westerhoff, I. G. Wisher, J. Wood, T. Yapici, G. B. Yodh, P. W. Younk, A. Zepeda, and H. Zhou, *Astrophys. J.* **843**, 39 (2017), [arXiv:1701.01778 \[astro-ph.HE\]](#).
- [37] R. Fleysher, L. Fleysher, P. Nemethy, A. I. Mincer, and T. J. Haines, *Astrophys. J.* **603**, 355 (2004), [arXiv:astro-ph/0306015 \[astro-ph\]](#).